

Photogrammetric techniques in multi-camera tomographic PIV

H.-G. Maas¹, P. Westfeld¹, T. Putze¹, N. Bøtkjær², J. Kitzhofer³, C. Brücker³

¹Institute of Photogrammetry and Remote Sensing, TU Dresden, D-01069 Dresden, Germany
 hans-gerd.maas@tu-dresden.de

²Dantec Dynamics A/S, DK-2740 Skovlunde, Denmark
 nicolas.boetkjaer@dantecdynamics.com

³Institute of Mechanics and Fluid Dynamics, TU Freiberg, D-09599 Freiberg, Germany
 bruecker@imfd.tu-freiberg.de

ABSTRACT

The paper presents several improvements to volumetric particle image velocimetry (PIV) with the goal of optimizing the efficiency and the flexibility of the method. An approach of sequential projective transformation of each camera image into each depth layer of the object voxel space, combined with a MinART (minstore algebraic reconstruction technique) is used for volumetric reconstruction. 3-D tracking is performed by 3-D least squares matching determining 12 parameters of a 3-D affine transformation between cuboids in successive voxel datasets. Besides the cuboid translation, these parameters also include information on the shear tensor of each cuboid.

1. INTRODUCTION

Elsinga *et al.* [1] have proposed an approach to 3-D PIV, which is based on a tomographic reconstruction of the observation volume and subsequent 3-D cross correlation in time-resolved voxel data. Tomographic PIV generates a tomographic reconstruction of a particle constellation from a limited number of camera views, for instance by applying Herman and Lent's [6] MART algorithm (multiplicative algebraic reconstruction technique). 3-D velocity field information can be obtained from time-resolved voxel data by dividing the data into cuboids of a pre-defined size and tracking these cuboids. Herein, 3-D cross correlation is a straightforward enhancement when advancing from 2-D PIV to 3-D PIV.

Disadvantages of both, MART and 3-D cross correlation can be seen in the computational effort causing rather long processing times. In the following, we will present an alternative efficient approach on volumetric reconstruction (Sec. 2) and a 12-parameter least squares approach for cuboid tracking in voxel data sequences (Sec. 3). In Sec. 4, we will present results obtained in the measurement of a vortex ring in a water tank.

2. VOLUMETRIC RECONSTRUCTION

As an alternative volumetric reconstruction technique, we developed a scheme based on a multiple projective transformation of each camera image contents into each depth layer of the object space [4] [5]. Compared to pixel-wise line-of-sight based implementations, this approach may save a considerable amount of computation time, especially if graphics card functionality can be used.

In a first step, a voxel structure of adequate resolution is defined in object space and initialized by setting the value of every voxel to 255. The reconstruction of the object space light intensity field is performed by transforming the content of each

camera image into each depth layer of the voxel space. Using homogeneous coordinates, a simple and fast computation can be performed. The relationship between the image coordinates \mathbf{x}' of a camera image and the voxel coordinates of a depth layer D_i in object space is

$$\mathbf{x}' = \mathbf{H}_i \cdot D_i \quad (1)$$

\mathbf{H}_i contains the 8 parameters of a projective transformation. For a first layer D_0 , the elements of \mathbf{H}_0 can be determined from the parameters of the exterior and interior orientation of the camera (projection center X_0, Y_0, Z_0 , 3×3 rotation matrix \mathbf{R} , camera constant c):

$$\mathbf{H}_0 = \begin{bmatrix} -c \cdot r_{11} & -c \cdot r_{21} & c \cdot (r_{11} \cdot X_0 + r_{21} \cdot Y_0 + r_{31} \cdot Z_0) \\ -c \cdot r_{12} & -c \cdot r_{22} & c \cdot (r_{12} \cdot X_0 + r_{22} \cdot Y_0 + r_{32} \cdot Z_0) \\ r_{13} & r_{23} & -r_{13} \cdot X_0 - r_{23} \cdot Y_0 - r_{33} \cdot Z_0 \end{bmatrix} \quad (2)$$

The transformation matrices \mathbf{H}_i of all further depth layers can be determined by adding an increment \mathbf{h}_i to \mathbf{H}_0 . Due to the parallelism of the depth layers, the determination of \mathbf{h}_i is simplified:

$$\mathbf{h}_i = \begin{bmatrix} 0 & 0 & -c \cdot r_{31} \cdot Z_i \\ 0 & 0 & -c \cdot r_{32} \cdot Z_i \\ 0 & 0 & r_{33} \cdot Z_i \end{bmatrix} \quad (3)$$

$$\mathbf{H}_i = \mathbf{H}_0 + \mathbf{h}_i \quad (4)$$

In homogeneous coordinates, it is sufficient to go through the transformation for the corner pixels of a layer only. All other gray values can be obtained by a bilinear interpolation.

After transforming the contents of the first camera image into the volumetric reconstruction space, the procedure is repeated for all other cameras. Obviously, each object space voxel will obtain different gray values from different views. The voxel space particle reconstruction is based on a simple assumption: A voxel belonging to a valid particle must have a high gray value in every image. This rule is realized by a multiplication of the gray values from each projection in the MART algorithm. The rule can be implemented even more efficiently by a minimum operator, where the gray value of a voxel GV is the minimum of its gray values in all views gv_j :

$$GV = \min \{gv_j\}, \quad gv_j \in \{0 \dots 255\} \quad (5)$$

Applying this MinART (minstore algebraic reconstruction technique), only those voxels, which get a high gray value from every view, will 'survive'. A 3-D particle constellation can then easily be obtained by a thresholding in voxel space. A background image derived from spatio-temporal histogram analysis is subtracted from each image beforehand to eliminate the effect of background reflections. In our approach we used four cameras, but the technique can be applied to an arbitrary number of views. The method may also be extended to the

use in liquids by integrating a ray tracing procedure into the multiple rectification approach or by using telecentric lenses.

3. 3-D LEAST SQUARES TRACKING

Eulerian 3-D velocity field information in time-resolved voxel space representations can be obtained by applying volume-based tracking methods. Here, 3-D least squares tracking (3-D LST) forms a rather interesting alternative to 3-D cross correlation. 3-D LST is a volumetric tracking technique, which is adaptive to cuboid deformation and rotation. It was first presented by Maas *et al.* [3] for tracking structures in 3-D LIF (laser induced fluorescence) data. It is formulated as an iterative least squares adjustment procedure, where the gray values of a cuboid g_1 at a time instance T_1 are transformed into the gray values of a cuboid g_2 at a time instance T_2 . The geometric transformation between the two cuboids is a 3-D affine transformation:

$$\begin{aligned} x_2 &= a_0 + a_1 x_1 + a_2 y_1 + a_3 z_1 \\ y_2 &= b_0 + b_1 x_1 + b_2 y_1 + b_3 z_1 \\ z_2 &= c_0 + c_1 x_1 + c_2 y_1 + c_3 z_1 \end{aligned} \quad (6)$$

In addition to the three cuboid translation vector components (a_0, b_0, c_0) , the 12 parameters of the 3-D affine transformation in 3-D LST contain scale, rotation and shear information for each cuboid. This allows for a higher precision especially in case of velocity gradients in the interrogation volume, as the cuboid shape is adapted. Moreover, these parameters enable the determination of a shear tensor for each interrogation cuboid. The 12 affine transformation parameters are obtained in an iterative manner, starting from approximate values and usually converging to the correct solution within a few iterations. Approximate values may be obtained from pre-knowledge on the flow or by hierarchically applying the technique on multiple resolution pyramid levels of the voxel data.

The least squares adjustment model in 3-D LST states the equality of two cuboids g_1 and g_2 , adding an error vector e to consider noise in the data:

$$g_1(x, y, z) - e(x, y, z) = g_2(x, y, z) \quad (7)$$

If only a translation (a_0, b_0, c_0) between the two cuboids is allowed, we get a linearized observation equation

$$g_1(x, y, z) - e(x, y, z) = g_2^0(x, y, z) + \frac{\partial g_2^0(x, y, z)}{\partial x} a_0 + \frac{\partial g_2^0(x, y, z)}{\partial y} b_0 + \frac{\partial g_2^0(x, y, z)}{\partial z} c_0 \quad (8)$$

wherein g_2^0 is the cuboid in the 2nd time instance at its initial approximate position and $(\partial g_2^0 / \partial x, \partial g_2^0 / \partial y, \partial g_2^0 / \partial z)$ are gray value gradients in the cuboid.

If the transformation is a 3-D affine transformation, we get

$$\begin{aligned} g_1(x, y, z) - e(x, y, z) &= g_2^0(x, y, z) \\ &+ \frac{\partial g_2^0(x, y, z)}{\partial x} dx + \frac{\partial g_2^0(x, y, z)}{\partial y} dy + \frac{\partial g_2^0(x, y, z)}{\partial z} dz \end{aligned} \quad (9)$$

with $dx = (\partial x / \partial d p_i) \cdot d p_i$, $dy = (\partial y / \partial d p_i) \cdot d p_i$, $dz = (\partial z / \partial d p_i) \cdot d p_i$, $p_i \in (a_0, a_1, a_2, a_3, b_0, b_1, b_2, b_3, c_0, c_1, c_2, c_3)$

With

$$g_x = \frac{\partial g_2^0(x, y, z)}{\partial x}, \quad g_y = \frac{\partial g_2^0(x, y, z)}{\partial y}, \quad g_z = \frac{\partial g_2^0(x, y, z)}{\partial z} \quad (10)$$

this leads to a linearized observation equation

$$\begin{aligned} g_1(x, y, z) - e(x, y, z) &= g_2^0(x, y, z) \\ &+ g_x da_0 + g_x x_2^0 da_1 + g_x y_2^0 da_2 + g_x z_2^0 da_3 \\ &+ g_y db_0 + g_y x_2^0 db_1 + g_y y_2^0 db_2 + g_y z_2^0 db_3 \\ &+ g_z dc_0 + g_z x_2^0 dc_1 + g_z y_2^0 dc_2 + g_z z_2^0 dc_3 \end{aligned} \quad (11)$$

Each voxel in a cuboid produces one observation equation. The complete equation system is solved in a Gauss-Markov estimation model determining the 12 transformation parameters in a way that the sum of the squares of gray value differences between the voxel of the two cuboids reaches a minimum.

The result of 3-D LST applied to sequences of tomographically reconstructed voxel structures is a dense 3-D velocity vector field with additional shear tensor information. When applied to liquid flow data, an incompressibility constraint is introduced to force the volume of a cuboid to remain constant during the iterative transformation.

As a least squares adjustment method, 3-D LST also delivers information on the precision, determinability and reliability of the 12 affine transformation parameters. This includes the standard deviation of each of the parameters as well as the correlation between parameters. This allows for the application of significance tests on each parameter in each cuboid to decide whether a transformation parameter is significant or not. In our approach, all non-significant parameters (except the three translation parameters) are set to zero and excluded. A more detailed description of 3-D LST can be found in [3].

4. PRACTICAL RESULTS

The tomographic reconstruction and cuboid tracking has been implemented and tested in the investigation of a vortex ring in a water tank. A volume of about $10 \times 10 \times 1 \text{ cm}^3$ is illuminated by a 3-D laser beam device and is recorded by a system of four 1024×1024 pixel high speed cameras equipped with telecentric lenses [2]. Neutrally buoyant seeding particles were injected into the center of the vortex generator. The experiments are performed with an image rate of 1000 frames/s.

The four-camera system was calibrated by taking image sequences of a target, which was moved through the observation volume by a 3-D translation stage. From these reference positions and their respective image coordinates, the orientation parameters of each camera were determined in a parallel projection telecentric optics camera model. The transition of the optical paths from the camera through the plain glass interface into the water could be neglected due to the fact that the cameras were equipped with telecentric lenses warranting a parallel projection rather than central perspective projection. Lens distortion was less than 0.5 pixel.

Figure 1 shows the four camera views of one epoch. From these images, a volumetric representation of $278 \times 1112 \times 944$ voxel was generated applying the technique as described in Sec. 2. Each voxel corresponds to $(90 \mu\text{m})^3$.

A regular grid of 25^3 voxel cuboids was defined into the volumetric reconstruction to apply the 3-D LST. For each cuboid, the 12 parameters of the 3-D affine transformation were determined as described in Sec. 3. Parameters, which turned out insignificant in the significance test, were excluded from the transformation. A volume constraint was applied to consider the incompressibility of the liquid. Outliers in the results were removed in a outlier detection procedure based on the following

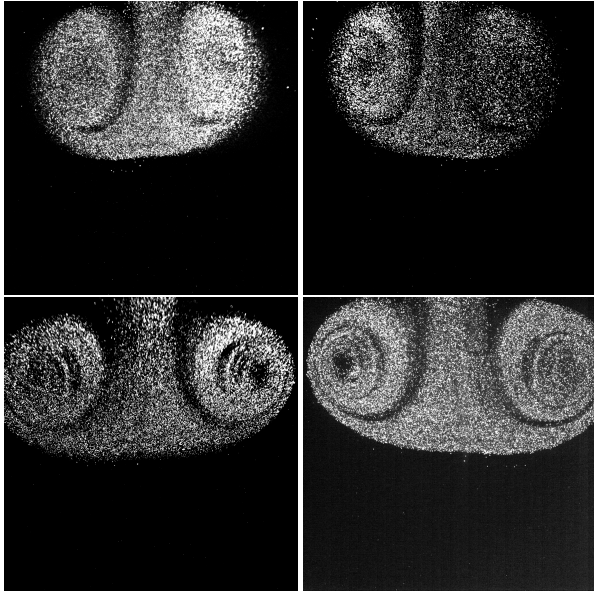


Figure 1: Vortex ring imaged with four high speed digital cameras equipped with telecentric lenses at one epoch.

criteria:

- Affine transformation parameter standard deviation: The standard deviations of the cuboid transformation parameters, which are part of the result delivered by 3-D LST, were analyzed. The results of those cuboids with standard deviations exceeding a preset threshold were deleted.
- Convergence behavior: 3-D LST is an iterative procedure, which usually converges after a few iterations. Cuboids with a diverging or oscillating solution were rejected.
- Vector length: Translation vectors exceeding a preset threshold were eliminated.
- Neighborhood correlation: The differences of the translation vector components between neighboring cuboids were analyzed. Vectors with deviations from their neighborhood exceeding a preset limit were eliminated.

The 3-D LST steering parameters were set on the basis of a-priori knowledge on the flow and empirically on the basis of a series of program runs. The parameters controlling the outlier elimination process were set automatically following 3-sigma rules. In total, 822 out of a total of 4908 ($b=17\%$) tracked cuboids were excluded for the first epoch for one half of the axis-symmetric vortex ring as shown in Figure 2 and 3. Herein, outliers are mainly situated in border regions of the vortex ring, and rather rigid outlier elimination criteria were applied. Optionally, gaps in the vector field can be closed by neighborhood based interpolation.

Figure 2 shows a color-coded visualization of selected layers in the 3-D LST results. Only the cuboid translation vectors are shown here. Table 1 lists the mean, minimum and maximum velocities obtained in this experiment. The vortex was generated in Z-direction with a speed of approximately 50 mm/s, but experience an acceleration within the ring due to induced velocity.

Figure 3 shows the translation vector lengths of one half of the vortex ring in a frontal view. As one can see, some velocity vectors in the centrum of the vortex were eliminated as potential outliers. This has to be attributed to the finite cuboid size

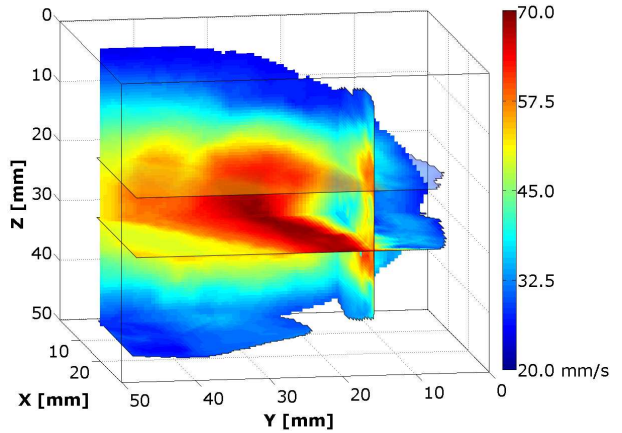


Figure 2: Cross sections of color-coded velocity in voxel space.

	v_x	v_y	v_z
mean	4.78	13.69	37.20
min	0.00	0.00	0.00
max	25.58	46.10	69.88

Table 1: Mean, minimum and maximum velocities (in mm/s).

and the fact that the 3-D affine transformation parameters can only recover linear cuboid deformations. The results might be improved by some parameter fine tuning or by a higher seeding density allowing for smaller cuboids.

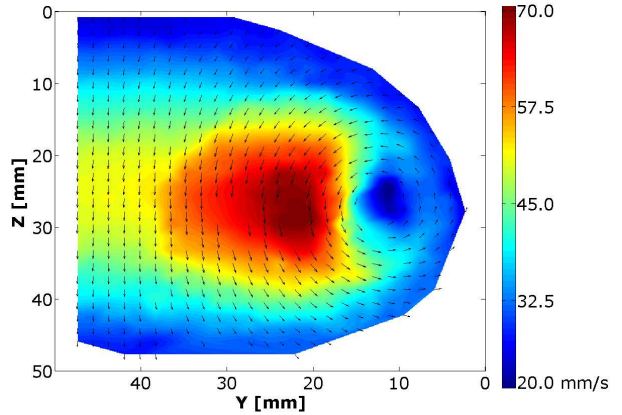


Figure 3: Color coded vector lengths of one half of the vortex ring (frontal view, $X=\text{const}=13.14$ mm).

Table 2 gives an overview on the percentage of significant 3-D affine transformation parameters over all accepted cuboids. As the cuboid translation parameters (a_0, b_0, c_0) were not excluded as a rule in the significance tests, they all have 100 % here. The scale parameters (a_1, b_2, c_3), constrained by the incompressibility condition, were only significant in relatively few cuboids, while the rotation and shear parameters ($a_2, a_3, b_1, b_3, c_1, c_2$) were significant especially in the center of the vortex (Figure 4). In total, about 20 % of the cuboids showed at least one significant non-translation parameter, proving the adequateness of the 3-D LST approach.

Besides the actual 3-D affine transformation parameters, 3-D LST also delivers the standard deviation of all transformation parameters. In the experiment described here, the standard deviation of unit weight produced by the least squared

a_0	b_0	c_0			
100	100	100			
a_1	b_2	c_3			
1.95	2.68	3.75			
a_2	a_3	b_1	b_3	c_1	c_2
4.42	10.47	6.40	10.77	6.07	12.61

Table 2: Percentage of significant parameters in accepted trajectories.

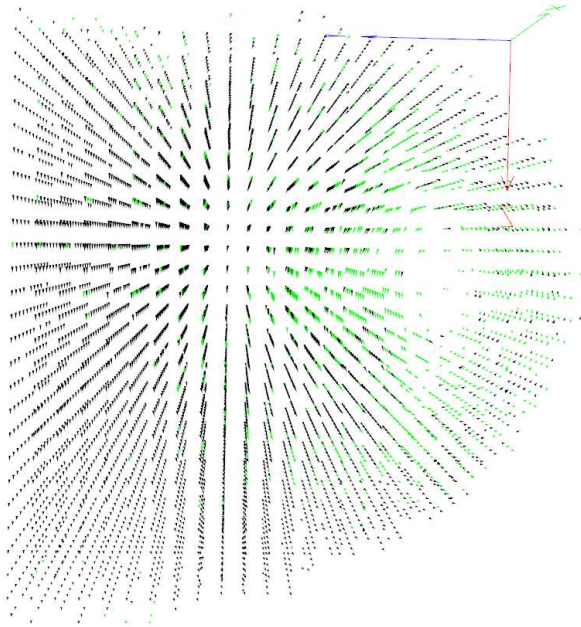


Figure 4: Velocity vector display with vectors belonging to cuboids with at least one significant non-translation 3-D affine transformation parameter coded in green.

adjustment process, averaged over all accepted cuboids, was 2.5 gray values. Table 3 shows the average standard deviations of the 12 affine transformation parameters. As one can see, the internal precision of the cuboid translation parameters is in the order of 1/100 of a voxel. However, one has to consider that these internal precision figures are only realistic if the assumed functional and stochastic model is correct (3-D affine transformation and least squares adjustment assuming Gaussian error distribution). Further verification tests have to be performed to get a better estimate of the real accuracy potential of the method.

a_0	b_0	c_0			
0.0132	0.0105	0.009			
a_1	b_2	c_3			
0.0024	0.0018	0.0016			
a_2	a_3	b_1	b_3	c_1	c_2
0.0024	0.0023	0.0017	0.0018	0.0016	0.0016

Table 3: Average standard deviations of transformation parameters (in voxel).

5. CONCLUSION

The suggested approach based on sequential projective transformation and 3-D least squares tracking turned out to be an efficient and accurate volumetric PIV technique. The

sequential projective transformation has the advantage of being fast and graphics card implementation friendly. 3-D LST as a cuboid tracking technique has the great advantage of inherently determining 12 affine transformation parameters of each cuboid. These 12 parameters allow to adapt to linear deformations of cuboids, thus improving the precision and reliability of cuboid translation parameters. Moreover, they form a basis for the determination of a shear tensor for each tracked cuboid. The fact that about 20 % of tracked cuboids in a vortex ring experiment showed at least one significant non-translation parameter, proves the relevance of determining not only transformation parameters in cuboid tracking.

Future work will concentrate on the optimization of the parametrization of the algorithms with the goal of achieving a maximum number of reliable velocity vectors and shear tensors. While in the experiment reported here, cubic interrogation areas have been used, a transition to oriented non-cubic cuboids, adapted to the flow pattern, will contribute to a reduction of the number of eliminated vectors. Beyond, the linear transformation model in 3-D LST can be extended by introducing higher order polynomials. The resolution of the velocity field may also be improved by identifying individual particles in voxel space and tracking those particles, using the results of the volume-based tracking as good approximation.

REFERENCES

- [1] Elsinga, G. E., Scarano, F., Wieneke, B. & van Oudheusden, B. W. (2005) Tomographic particle image velocimetry. In *6th International Symposium on Particle Image Velocimetry (PIV05)*.
- [2] Kitzhofer, J., Kirmse, C. & Brücker, C. (2009) High density, long-term 3d ptv using 3d scanning illumination and telecentric imaging. In W. Nitsche and C. Dobriloff, editors, *Imaging Measurement Methods for Flow Analysis*, Volume 106/2009 of Notes on Numerical Fluid Mechanics and Multidisciplinary Design, pages 125134. Springer Berlin / Heidelberg. doi: 10.1007/978-3-642-01106-1.
- [3] Maas, H.-G., Stefanidis, A. & Grün, A. (1994) From pixels to voxels - tracking volume elements in sequences of 3-d digital images. In *International Archives of Photogrammetry and Remote Sensing*, Volume 30, 3/2.
- [4] Maas, H.-G., Putze, T. & Westfeld, P. (2009) Recent developments in 3d-ptv and tomo-piv. In W. Nitsche and C. Dobriloff, editors, *Imaging Measurement Methods for Flow Analysis*, Volume 106/2009 of Notes on Numerical Fluid Mechanics and Multidisciplinary Design, pages 53-62. Springer Berlin / Heidelberg. doi: 10.1007/978-3-642-01106-1.
- [5] Putze, T. & Maas, H.-G (2008) 3D determination of very dense particle velocity fields by tomographic reconstruction from four camera views and voxel space tracking. In Jiang J. Chen J. and H.-G. Maas, editors, *International Archives of Photogrammetry, Remote Sensing and Spatial Information Sciences*, Volume XXXVII, Part B5, pages 33-38. ISPRS.
- [6] Herman, G. T. & Lent, A. (1976) Iterative reconstruction algorithms. *Computers in Biology and Medicine*, 6:273-294.